

# BLIND ITERATIVE RESTORATION OF IMAGES WITH SPATIALLY-VARYING BLUR

John Bardsley <sup>\*</sup>  
Stuart Jefferies <sup>†</sup>  
James Nagy<sup>‡</sup>  
Robert Plemmons<sup>§</sup>

## ABSTRACT

Removing non-uniform blur and noise from optical images is a very difficult problem to resolve. In this paper we describe a strategy that can be used for solving such problems. We describe how to restore images blurred by an unknown spatially-varying point spread function (PSF) by using a combination of methods including sectioning and phase diversity blind deconvolution. The PSFs on the individual sections are not known in advance. We treat the sections as a sequence of frames whose PSFs are correlated and approximately spatially-invariant, and apply iterative blind deconvolution schemes based on phase diversity to approximate these PSFs. A technique by Nagy and O’Leary is then used to restore the image globally. Test results on star cluster data are presented.

## 1. INTRODUCTION

To establish some initial notation, we model the basic image restoration problem as:

$$g = Sf + \eta, \tag{1.1}$$

where  $g$  is the blurred, noisy image,  $f$  is the unknown true image,  $\eta$  is additive noise, and  $S$  is a matrix modelling the blurring operation. In the case of spatially invariant blurs,  $Sf$  is usually written as a convolution of the associated point spread function (PSF)  $s$  and the object  $f$ . However, if the blur is spatially variant,  $Sf$  cannot be written as a simple convolution operation, and thus the restoration problem is much more difficult.

In this paper we describe a strategy for solving such problems. We describe how to restore images blurred by an unknown spatially-varying point spread function (PSF) by using a combination of methods including sectioning and phase diversity-based blind deconvolution. The PSFs on the individual sections are not known in advance. We treat the sections as a sequence of frames whose PSFs are correlated and approximately spatially-invariant, and apply iterative blind deconvolution schemes based on phase diversity to approximate these PSFs. A technique by Nagy and O’Leary<sup>10</sup> is then used to restore the image globally.

In Section 2 we describe our use of phase diversity-based blind deconvolution to estimate the PSFs in regions of the segmented image. The segmentation process and a global restoration scheme are given in Section 3. Results on some tests using simulated star field images taken through atmospheric turbulence are provided in Section 4, while conclusions and comments on the spatially-varying blur removal problem are given in Section 5.

---

<sup>\*</sup>Department of Mathematical Sciences University of Montana, Missoula, MT 59812. Research supported in part by University of Montana Research Grant MRA682.

<sup>†</sup>Maui Scientific Research Center, University of New Mexico, 590 Lipoa Parkway, Kihei, HI, and Stewart Observatory, University of Arizona, Tuscon, AZ 85721. Research supported in part by the Air Force Office of Scientific Research under grant F49620-02-1-0107.

<sup>‡</sup>Department of Mathematics and Computer Science, Emory University, Atlanta, GA 30322. Research supported in part by the NSF under grant DMS-05-11454 and by an Emory University Research Committee grant.

<sup>§</sup>Department Computer Science, Wake Forest University, Winston-Salem, NC 27109. Research supported in part by the Air Force Office of Scientific Research under grant F49620-02-1-0107, by the Army Research Office under grants DAAD19-00-1-0540 and W911NF-05-1-0402, and by UT-Battelle under Contract No. DE-AC05-00OR22725, with funding from ARDA.

## 2. APPROXIMATING PSFS BY PHASE DIVERSITY

As discussed in, e.g.,<sup>17</sup> with atmospheric turbulence the phase varies both with time and position in space. Adaptive optics systems use deformable mirrors to correct for these phase variations. Errors in this correction process arise from a variety of sources, e.g., errors in the measurement of phase, inability of the mirror to conform exactly to the phase shape, and lag time between phase measurement and mirror deformation. Thus, a spatially variant model can potentially produce better restorations.

In this section we describe a phase diversity-based scheme to approximate the PSF associated with each section of a segmented image. For a sufficiently fine segmentation, the PSF can be assumed to be essentially spatially invariant, and thus a blind deconvolution scheme can be applied. The mathematics of this phase recovery process was first described by Gonsalves,<sup>7</sup> and has been applied extensively for imaging through atmospheric turbulence.<sup>15</sup>

Assuming that light emanating from the object is incoherent, the dependence of the PSF on the phase is given by

$$s[\phi] = |\mathcal{F}^{-1}(pe^{i\phi})|^2, \quad (2.2)$$

where  $p$  denotes the pupil, or aperture, function,  $i = \sqrt{-1}$ , and  $\mathcal{F}$  denotes the 2-D Fourier transform,

$$(\mathcal{F}h)(\mathbf{y}) = \int \int_{\mathbb{R}^2} h(\mathbf{x}) e^{-i2\pi \mathbf{x} \cdot \mathbf{y}} d\mathbf{x}, \quad \mathbf{y} \in \mathbb{R}^2. \quad (2.3)$$

The pupil function  $p = p(x_1, x_2)$  is determined by the extent of the telescope's primary mirror. In phase diversity-based blind deconvolution, the  $k^{\text{th}}$  diversity image is given by

$$d_k = s[\phi + \theta_k] \star f + \eta_k, \quad k = 1, \dots, K, \quad (2.4)$$

where  $\eta_k$  represents noise in the data,  $f$  is the unknown object,  $s$  is the point spread function (PSF),  $\phi$  is the unknown phase function,  $\theta_k$  is the  $k^{\text{th}}$  phase diversity function, and  $\star$  denotes convolution product,

$$(s \star f)(\mathbf{x}) = \int \int_{\mathbb{R}^2} s(\mathbf{x} - \mathbf{y}) f(\mathbf{y}) d\mathbf{y}, \quad \mathbf{x} \in \mathbb{R}^2. \quad (2.5)$$

Here,  $s[\phi]$ , given in (2.2), is the PSF denoted by  $s$  earlier, and is represented by the matrix  $S$  in (1.1).

In atmospheric optics,<sup>15</sup> the phase  $\phi(x_1, x_2)$  quantifies the deviation of the wave front from a reference planar wave front. This deviation is caused by variations in the index of refraction (wave speed) along light ray paths, and is strongly dependent on air temperature. Because of turbulence, the phase varies with time and position in space and is often modelled as a stochastic process.

Additional changes in the phase  $\phi$  can occur after the light is collected by the primary mirror, e.g., when adaptive optics are applied. This involves mechanical corrections obtained with a deformable mirror to restore  $\phi$  to planarity. By placing beam splitters in the light path and modifying the phase differently in each of the resulting paths, one can obtain more independent data. The phase diversity functions  $\theta_k$  represent these deliberate phase modifications applied *after* light is collected by the primary mirror. The easiest to implement is *defocus blur*, modelled by a quadratic

$$\theta_k(x_1, x_2) = b_k (x_1^2 + x_2^2), \quad (2.6)$$

where the parameters  $b_k$  are determined by defocus lengths. In practice, the number of diversity images is often quite small, e.g.,  $K = 2$  in the numerical simulations to follow. In addition, one of the images, which we will denote using index  $k = 1$ , is obtained with no deliberate phase distortion, i.e.,  $\theta_1 = 0$  in (2.4).

## 2.1. Formulating and Solving the Optimization Problem

To estimate the phase  $\phi$ , and the object  $f$  from data (2.4), we consider the least squares fit-to-data functional

$$J_{data}[\phi, f] = \frac{1}{2K} \sum_{k=1}^K \|s[\phi + \theta_k] \star f - d_{k,t}\|^2. \quad (2.7)$$

Here  $\|\cdot\|$  denotes the standard  $L^2$  norm. Since deconvolution and phase retrieval are both ill-posed problems, any minimizer of  $J_{data}$  is unstable with respect to noise in the data. Hence we add regularization terms to obtain the *full cost functional*,

$$J_{full}[\phi, f] = J_{data}[\phi, f] + \gamma J_{object}[f] + \alpha J_{phase}[\phi]. \quad (2.8)$$

Here the regularization parameters  $\gamma$  and  $\alpha$  are positive real numbers, and the regularization functionals  $J_{object}$  and  $J_{phase}$  provide stability and incorporate prior information.

Because of atmospheric turbulence, variations in the refractive index, and hence the phase itself, can be modelled as a random process.<sup>15</sup> We apply the von Karman turbulence model, which assumes this process is second order, wide sense stationary, and isotropic with zero mean. It can be characterized by its power spectral density,

$$\Phi(\omega) = \frac{C_1}{(C_2 + |\omega|^2)^{11/6}}, \quad (2.9)$$

where  $\omega = (\omega_x, \omega_y)$  represents spatial frequency. Corresponding to this stochastic model for phase, we take the phase regularization functional

$$J_{phase}[\phi] = \frac{1}{2} \langle \Phi^{-1} \mathcal{F}\{\phi\}, \mathcal{F}\{\phi\} \rangle, \quad (2.10)$$

where  $\langle f, g \rangle = \int_{-\infty}^{\infty} \int_{-\infty}^{\infty} f(\omega) g^*(\omega) d\omega$ , and the superscript  $*$  denotes complex conjugate. For regularization of the object, we take the “minimal information prior”

$$J_{object}[f] = \frac{1}{2} \|f\|^2. \quad (2.11)$$

Note that the object regularization functional (2.11) is quadratic and the dependence of the fit-to-data functional (2.7) on the object  $f$  is quadratic. Moreover, the Hessian with respect to the object of the full cost functional (2.8) is symmetric and positive definite with eigenvalues bounded below by  $\gamma$ . By setting the gradient with respect to the object equal to zero, one obtains a linear equation whose solution yields the object at a minimizer for  $J_{full}$ .<sup>14</sup> Using the convolution theorem together with the fact that the Fourier transform preserves the  $L^2$  norm, one obtains the Fourier representation for the minimizing object,

$$F = \frac{P[\phi]^*}{Q[\phi]}, \quad (2.12)$$

where

$$P[\phi] = \sum_k D_k^* S_k[\phi], \quad Q[\phi] = \gamma + \sum_k |S_k[\phi]|^2. \quad (2.13)$$

Here  $F = \mathcal{F}\{f\}$ ,  $D_k = \mathcal{F}\{d_k\}$ , and  $S_k[\phi] = \mathcal{F}\{s[\phi + \theta_k]\}$ . Substituting (2.12) back into (2.8), one obtains the cost functional that we will minimize,

$$J[\phi] = J_{reduced\ data}[\phi] + \alpha J_{phase}[\phi], \quad (2.14)$$

where

$$J_{reduced\ data}[\phi] = \sum_k \|D_k\|^2 - \left\langle \frac{P[\phi]}{Q[\phi]}, P[\phi] \right\rangle. \quad (2.15)$$

See Appendix B of<sup>17</sup> for a detailed derivation.

Our objective is to minimize (2.14) in order to obtain a reconstruction of the phase  $\phi$ . In order to do that, we need an effective computational method. For that purpose, we use a quasi-Newton, or secant, method known as limited memory BFGS (L-BFGS).<sup>12</sup> For details on the implementation of L-BFGS for minimizing (2.14) see.<sup>6</sup> The preconditioner used for the L-BFGS iterations is given by

$$M_\nu \psi = \mathcal{F}^{-1} (\Phi^{-1} \mathcal{F}(\psi)),$$

where  $\Phi$  is defined in (2.9).

Before continuing, we make the observation that the above computational approach provides estimates of both the phase  $\phi$  and object  $f$  (via (2.12)). In our application of removing spatially-varying blur, the main interest is in using this approach for obtaining the PSF as a function of the phase, as given in (2.2). The object  $f$  is then reconstructed in a second stage, which we now discuss.

### 3. SECTIONING THE IMAGE AND APPLYING A GLOBAL RESTORATION SCHEME

For many spatially variant blurs, in small regions of the image the blur can be well approximated by a spatially invariant PSF. This property has motivated several types of *sectioning methods*<sup>1,5,16</sup> that partition the image, restoring each local region using its corresponding spatially invariant PSF. The results are then sewn together to obtain the restored image. To reduce blocking artifacts at the region boundaries, larger, overlapping regions are used, and then the restored sections are extracted from their centers. Trussell and Hunt<sup>16</sup> proposed using the Landweber iteration for the local deblurring, and suggested a complicated stopping criteria based on a combination of local and global convergence constraints. Fish, Grochmalicki and Pike<sup>5</sup> use a truncated singular value decomposition (TSVD) to obtain the local restorations.

An alternative scheme can be derived by partitioning the image into subregions on which the blur is assumed to be spatially invariant; but, rather than deblurring the individual subregions locally and then sewing the individual results together, we first sew (interpolate) the individual PSFs, and restore the image globally. In algebraic terms, the blurring matrix  $S$ , given in (1.1), can be written as

$$S = \sum_{i=1}^p \sum_{j=1}^p D_{ij} S_{ij}, \quad (3.16)$$

where  $S_{ij}$  a matrix representing the spatially invariant PSF in region  $(i, j)$ , and  $D_{ij}$  is a nonnegative diagonal matrix satisfying  $\sum \sum D_{ij} = I$ . For example, if piecewise constant interpolation is used, then the  $l$ th diagonal entry of  $D_{ij}$  is 1 if the  $l$ th point is in region  $(i, j)$ , and 0 otherwise.

Faisal et al.<sup>3</sup> use this formulation of the spatially variant PSF, apply the Richardson-Lucy algorithm with piecewise constant interpolation of the PSFs, and discuss a parallel implementation. Boden et al.<sup>2</sup> also describe a parallel implementation of the Richardson-Lucy algorithm, and consider piecewise constant as well as piecewise linear interpolation. Nagy and O'Leary<sup>11</sup> use a conjugate gradient algorithm with piecewise constant and linear interpolation, and also suggest a preconditioning scheme (for both interpolation methods) that can substantially improve the rate of convergence. Furthermore, in<sup>10</sup> they provide very efficient FFT-based algorithms.

Note that, using (3.16), the image formation model can be written as:

$$g = \sum_{i=1}^p \sum_{j=1}^p D_{ij} (s_{ij} \star f) + n, \quad (3.17)$$

where  $s_{ij}$  is the PSF for region  $(i, j)$ . This model assumes the PSFs are known, so the question is how to use this for blind deconvolution. The algorithm proceeds follows:

1. First determine a region  $(i, j)$  for which a good estimate of the PSF can be obtained. Use the L-BFGS method discussed in Section 2 on an extended region of  $(i, j)$  to obtain reconstruction of the phase  $\phi$  in that region. From  $\phi$  an approximation of the spatially invariant PSF for that region is obtained via (2.2). A reconstruction of the image contained in that region, if desired, could be computed by applying the inverse Fourier transform to  $F$  given in (2.12).
2. Now, assuming that the overall space varying PSF varies slowly across the image, the PSFs for the regions neighboring region  $(i, j)$  should be similar to the one in region  $(i, j)$ . That is, PSF  $s_{ij}$  should be a good estimate of the PSFs  $s_{i,j+1}$ ,  $s_{i,j-1}$ ,  $s_{i+1,j}$  and  $s_{i-1,j}$ . Thus, one can use  $\phi_{ij}$  for the initial guess  $\phi_0$  in the L-BFGS iterations, obtaining reconstruction for the phase, and image if desired. Once again, via (2.2), a reconstruction of the PSF is obtained.
3. Execute steps 1 and 2 for each region. When done, one hopefully has a set of good PSFs, and restored regions of the image. A global image restoration algorithm, with the individual (good) PSFs, can be used to restore the blurred image (as done by Nagy and O’Leary<sup>11</sup>). Note that the restored images in the regions can be pieced together, and used as an initial guess for the global restoration scheme.

#### 4. NUMERICAL EXAMPLES

In this section we describe some numerical experiments to illustrate the potential advantages of the space variant approach discussed in this paper. All tests were done on a simulated star field image, shown in Figure 1, which was obtained from the Space Telescope Science Institute ([www.stsci.edu](http://www.stsci.edu)).

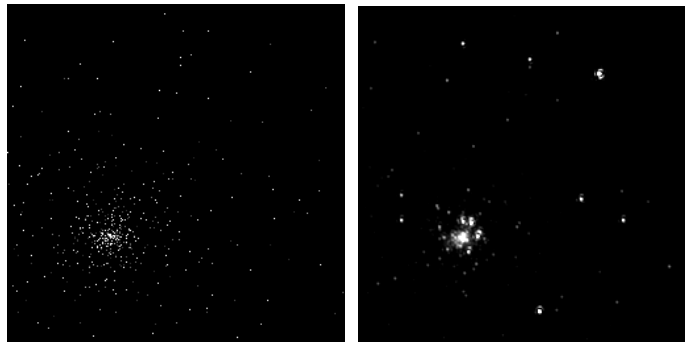


**Figure 1:** Simulated image of a star field. The true image is on the left, and the blurred noisy image is on the right.

To simulate an image blurred by a spatially variant point spread function, we begin by generating 1024 different PSFs. The PSFs were created by generating a single pupil function and a moving phase screen, each on a  $32 \times 32$  grid. Figure 2 shows the pupil function, two selected phase screens, and their corresponding PSFs.

The blurred image, shown in Figure 1, was then created by convolving each of the 1024 PSFs with successive  $32 \times 32$  pixels of the true image. By overlapping these regions, we obtain successive  $8 \times 8$  pixel regions of the blurred image with virtually no blocking (boundary) artifacts; see Figure 1. We use phase diversity, with one frame and two channels. The blind deconvolution (BD) algorithm we use is described in Section (2). Our regularization parameters were taken to be  $\alpha = 1 \times 10^{-1}$  and  $\gamma = 1 \times 10^{-4}$ . We stopped L-BFGS iterations once the norm of the gradient had been reduced by six orders of magnitude in all cases. This approach was used to reconstruct the PSFs in several situations:

- The algorithm is run using the whole blurred image, so we obtain a single PSF which represents a spatially invariant approximation of the spatially variant blurring operator.

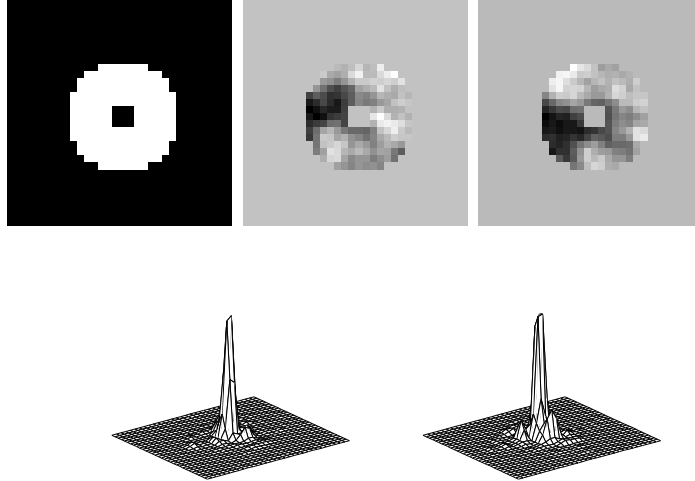


**Figure 2:** Pupil function (left), two sample phases and their corresponding PSFs.

- Next we section the image into 4 equally sized regions (that is, we use a  $2 \times 2$  partitioning of the image), and obtain 4 PSFs to construct an approximation of the space variant blur, as described in Section 3.
- Analogously, use a  $4 \times 4$  partitioning of the image to construct 16 PSFs to approximate the space variant blurring operator.
- Finally, we use a  $16 \times 16$  partitioning of the image to obtain 64 PSFs for the space variant approximation.

Once the PSFs are computed from the BD algorithm, we then use the conjugate gradient (CG) algorithm to reconstruct the image. Efficient implementation of the matrix vector multiplications for the space variant cases (4 PSFs, 16 PSFs, and 64 PSFs) was done using the approach outlined in Section 3. Goodness of fit is measured using the relative error,

$$\frac{\|f_{\text{true}} - f_k\|_2}{\|f_{\text{true}}\|_2}$$

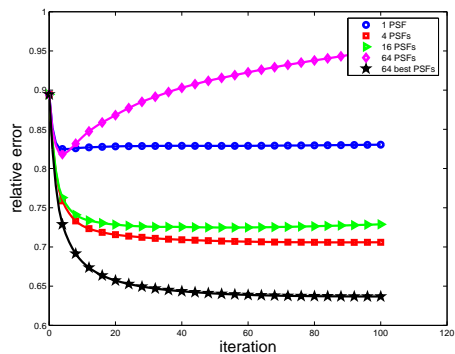
where  $f_{\text{true}}$  is the (diffraction limited) true image, and  $f_k$  is the (diffraction limited) solution at the  $k$ th CG iteration.

Figure 3 shows plots of the relative errors when no noise is added to the data. At first glance these appear to be disappointing results; 4 PSFs produce lower relative errors than a single PSF, but additional PSFs actually increase the relative error. It is important to note, however, that to obtain more PSFs, the blind deconvolution algorithm must be implemented on small regions of the image. If the small regions do not contain significant object information, then we cannot hope to obtain good approximations of the PSFs. Consequently, given the fact that the object that we are using in our experiment has significant black background, it is not surprising that several such small regions occur. Thus the poor results when using 64 PSFs.

On the other hand, some of the small regions may contain enough significant object information so that the blind deconvolution algorithm can reconstruct good PSFs. This motivates us to consider the following approach to construct 64 PSFs: Compute PSFs using successively small regions, and choose the ones that produce the best results. That is, we use a “mix” of PSFs computed by the various partitionings of the image. We used such an approach by looking first at the smallest regions (the 64 PSFs). If a PSF in a particular region was poor, then it was replaced by a PSF computed on a larger region. In order to have a systematic approach for choosing a good PSF, we compared the computed PSFs with the average PSFs described in the previous subsection. Of course in a realistic problem the average PSFs will not be available, and some other mechanism must be used to decide on the quality of the computed PSFs. In any case, our systematic approach shows that if the best

computed PSFs can be found, then substantially better reconstructions can be obtained; see the bottom curve in Figure 3. The reconstructed images are shown in Figure 4.

Similar results are obtained with noisy data. For example, with Poisson and Gaussian noise (mean 0, standard deviation 2) added to the blurred image, the relative errors using the CG iterative method are shown in Figure 5 and the corresponding reconstructions are shown in Figure 6.



**Figure 3.** Relative errors at each iteration of the conjugate gradient method, using increasingly more accurate approximations of the spatially variant blur. The PSFs used to approximate the space variant blur were computed using phase diversity-based blind deconvolution. These results were computed using noise free blurred image data.

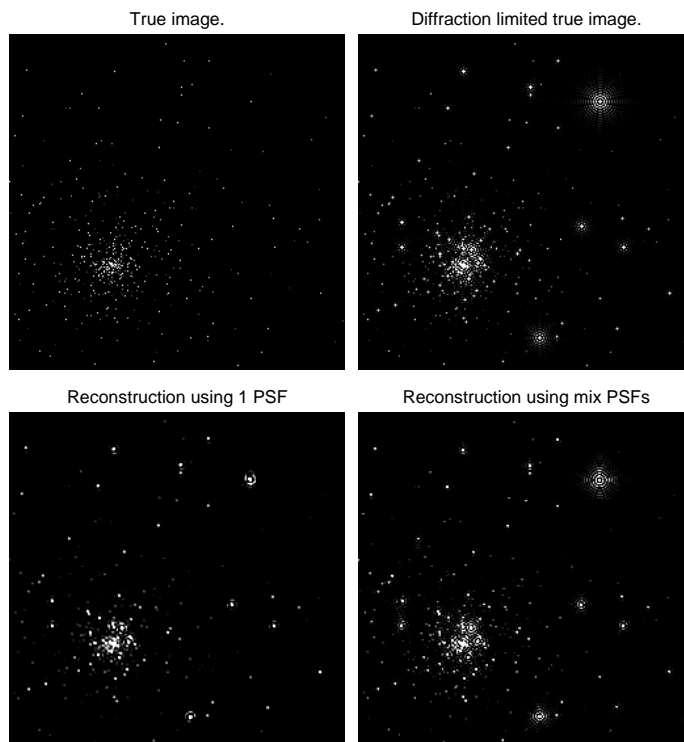


**Figure 4.** Reconstructions computed by the conjugate gradient algorithm. These results were obtained using PSFs computed from a phase diversity blind deconvolution algorithm. The blurred image data in this case is noise free.

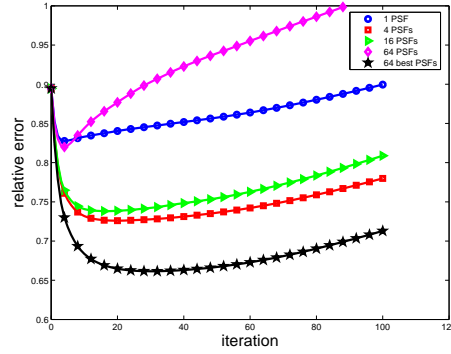


**Figure 5.** Relative errors at each iteration of the conjugate gradient method, using increasingly more accurate approximations of the spatially variant blur. The PSFs used to approximate the space variant blur were computed using phase diversity-based blind deconvolution. The results were computed from a noisy (Poisson and Gaussian) blurred image.

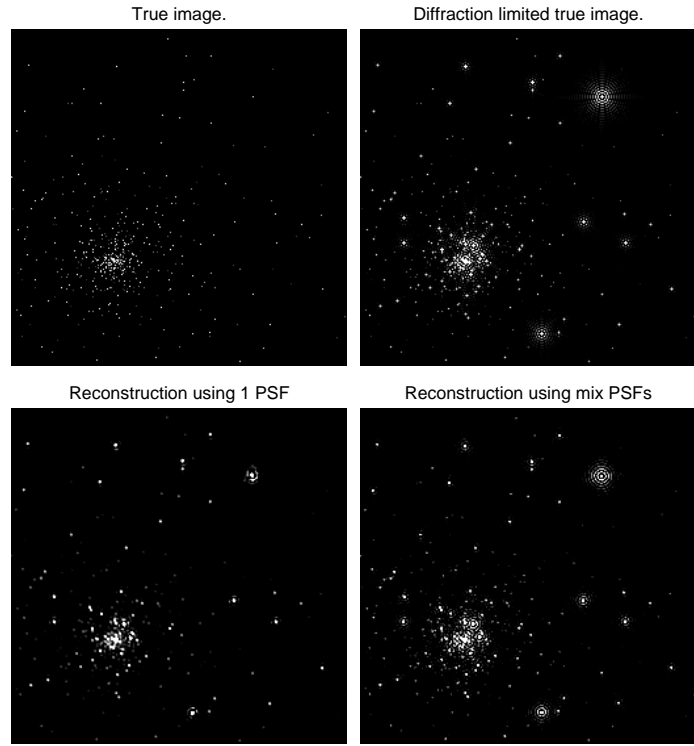


**Figure 6.** Reconstructions computed by the conjugate gradient algorithm. These images were obtained using PSFs computed from a phase diversity-based blind deconvolution algorithm. The results were computed from a noisy (Poisson and Gaussian) blurred image.

### 5. CONCLUSIONS

We have presented a computational approach for solving image restoration problems in which the blur in the image is both unknown and spatially varying. The approach has three stages. The first stage involves sectioning the image into regions in which the blur is believed to be approximately spatially invariant. In the second stage, phase diversity-based blind deconvolution via the L-BFGS optimization algorithm is implemented in order to obtain an estimate of the phase in each region. From these reconstructed phases, the corresponding PSF in each

region can be computed. In the final stage, with these PSFs in hand, the object can be reconstructed globally via the algorithm of Nagy and O’Leary.

Our numerical experiments show, first, that using a spatially varying model when a spatially varying blur is present does indeed provide more accurate results. Secondly, we find that in regions with little object information, the phase, and hence, PSF, reconstructions can be inaccurate. This motivates a “PSF mixing” approach, in which the object is divided into further subregions only in areas in which there is enough object information. Finally, our results show that our approach is very effective. A conclusion of particular importance that follows from our numerical experiments is that in the presence of an unknown, spatially varying blur, our approach is much more effective than is standard one-PSF phase-diversity.

## REFERENCES

1. H.-M. Adorf. Towards HST restoration with space-variant PSF, cosmic rays and other missing data. In R. J. Hanisch and R. L. White, editors, *The Restoration of HST Images and Spectra II*, pages 72–78, 1994.
2. A. F. Boden, D. C. Redding, R. J. Hanisch, and J. Mo. Massively parallel spatially-variant maximum likelihood restoration of Hubble Space Telescope imagery. *J. Opt. Soc. Am. A*, 13:1537–1545, 1996.
3. M. Faisal, A. D. Lanterman, D. L. Snyder, and R. L. White. Implementation of a modified Richardson-Lucy method for image restoration on a massively parallel computer to compensate for space-variant point spread function of a charge-coupled device camera. *J. Opt. Soc. Am. A*, 12:2593–2603, 1995.
4. D. Fish, A. Brinicombe, R. Pike, and J. Walker “Blind deconvolution by means of the Richardson-Lucy algorithm,” *J. Optical Soc. Amer. A*, Vol. 12, no. 1, pp. 58–65, 1995.
5. D. A. Fish, J. Grochmalicki, and E. R. Pike. Scanning singular-value-decomposition method for restoration of images with space-variant blur. *J. Opt. Soc. Am. A*, 13:1–6, 1996.
6. Luc Gilles, C. R. Vogel, J. M. Bardsley, *Computational Methods for a Large-Scale Inverse Problem Arising in Atmospheric Optics*, Inverse Problems, **18** (2002), pp. 237-252.
7. R. Gonsalves. Phase retrieval and diversity in adaptive optics. *Optical Engineering*, 21:829–832, 1982.
8. S. M. Jefferies and J. Christou, “Restoration of astronomical images by iterative blind deconvolution,” *The Astrophysical Journal*, Vol. 415, pp. 862–874, 1993.
9. K. P. Lee, J. Nagy, and L. Perrone, “Iterative methods for image restoration: A Matlab object oriented approach,” Preprint May 2002. Available from J. Nagy’s web page at: <http://www.mathcs.emory.edu/>.
10. J. G. Nagy and D. P. O’Leary. Fast iterative image restoration with a spatially varying PSF. In F. T. Luk, editor, *Advanced Signal Processing Algorithms, Architectures, and Implementations VII*, volume 3162, pages 388–399. SPIE, 1997.
11. J. Nagy and D. P. O’Leary, “Restoring images with spatially varying blur” , *SIAM J. Scientific Computing*, Vol. 19, pp. 1062–1083, 1998.
12. J. Nocedal and S. J. Wright, *Numerical Optimization*, Springer-Verlag, 1999.
13. J. Nagy, P. Pauca, R. Plemmons, and T. Torgersen, “Space-varying restoration of optical images,” *J. Optical Soc. Amer. A.*, Vol. 14, pp. 3162–3174, 1997.
14. R. Paxman, T. Schulz, and J. Fienup, *Joint estimation of object and aberrations by using phase diversity*, *J. Opt. Soc. Am. A*, **9** (1992), pp. 1072–1085.
15. M. C. Roggeman and B. Welsh, *Imaging Through Turbulence*, CRC Press, 1996.
16. H. J. Trussell and B. R. Hunt. Image restoration of space-variant blurs by sectional methods. *IEEE Trans. Acoust. Speech, Signal Processing*, 26:608–609, 1978.
17. C. R. Vogel, T. Chan, and R. J. Plemmons. Fast algorithms for phase diversity-based blind deconvolution. In *Adaptive Optical System Technologies*, Volume 3353. SPIE, 1998.